

# CONTRIBUTIONS OF AUTOIONIZING STATES TO THE NEAR-THRESHOLD ELECTRON IMPACT IONIZATION CROSS-SECTION OF SELENIUM ATOMS

A.A.Borovik (Jr.)<sup>1</sup>, F.F.Chipev<sup>2</sup>

<sup>1</sup>Uzhhorod National University, Voloshyna Str. 54, Uzhhorod, 88000  
e-mail: alex@aborovik.uzhgorod.ua

<sup>2</sup>Institute of Electron Physics, Ukrainian National Academy of Sciences,  
Universytetska Str. 21, Uzhhorod, 88017  
e-mail: dep@mail.uzhgorod.ua

A crossed electron and atomic beams scattering geometry was employed to measure ionization cross-section for selenium atoms from the threshold up to 19.2 eV with an energy resolution of 0.4 eV. For the first time a strong structure was revealed just above the ionization threshold and for the higher energies. Identification of the structure revealed the dominant role of dipole forbidden autoionizing configurations  $s^2p^3(^2D, ^2P)nl$  and  $sp^4(^4P)nl$  in the enhancement of the ionization cross-section (up to 19 %) in the impact energy range 13–15 eV. The evident resonance character of the structure points out the presence of negative-ions in the near-threshold excitation of the contributing autoionizing states.

## Introduction

An important role of autoionization in the impact ionization of atoms has been established earlier for all heavy alkali and alkaline-earth metals (see e.g. [1, 2] and references therein). The recent high-resolution studies have revealed the resonance character of the autoionization contribution in sodium [3], zinc [4], cadmium [5], magnesium [6] and potassium [7]. As it follows from these data, the presence of strong autoionization processes limits essentially the validity of the Wannier law even for the low- $Z$  atoms. The resonance character of the autoionization contribution points out an important role of negative ions in the near-threshold excitation of low-energy autoionizing states.

Excitation of the  $4p^4$  valence subshell of selenium leads to the formation of  $nd$  and  $ns$  single-electron Rydberg series converging to the  $4s^24p^3\ ^2D^0_{5/2,3/2}$  and  $4s^24p^3\ ^2P^0_{3/2,1/2}$  ionization limits [8, 9]. Electron decay of these levels may contribute to the single ionization cross-section in the impact energy region 9.8–12.5 eV. No transitions from the  $4p^4$

subshell were observed in selenium above this energy region. As to the excitation of the inner  $4s^2$  subshell, the  $4s4p^4np$  series was only observed in photoionization spectrum of selenium [9]. Five members of this series are located in two regions between 10–12 and 17–20 eV. To our knowledge, there are no data on the observation of autoionizing levels in selenium in the energy range 12.2–17.9 eV.

The first measurements of electron impact ionization of selenium were performed with an energy resolution of 0.5 eV over the impact energy range from the threshold up to 200 eV [10]. However, this work was devoted mainly to the task of absolute ionization cross-sections and the effect of autoionization was out of consideration.

As part of our current studies on electron-impact near-threshold ionization of complex atoms, we report the first data on the resonance structure observed in electron impact ionization cross-section of selenium in an impact energy region from the threshold up to 19.2 eV. Identification of the structure with the electron decay of autoion-

izing states was performed on the base of known photoionization data [8, 9].

### Apparatus

A crossed electron and atomic beams scattering geometry was employed to measure the ionization cross-section for selenium atoms (see Fig.1). The apparatus used in the measurements was similar to that described in details earlier [11]. Briefly, it consisted of an electron monochromator, an atomic beam source, and an ion detector. As a monochromator of incident electrons, a hypocycloidal analyzer with two sets of focusing apertures  $A_1$ – $A_2$ ,  $A_3$ – $A_4$  was used for producing the incident electron beam with an energy spread better than 0.4 eV (FWHM) over an energy range of 0.1–15 eV. The measurements were performed at a typical intensity of the electron beam of  $10^{-7}$  A.

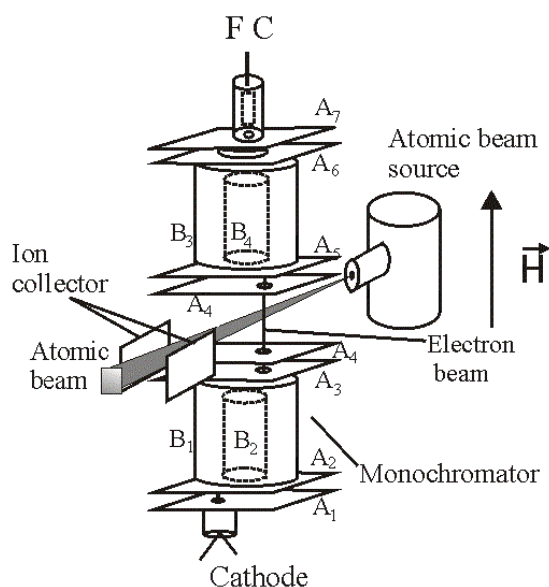


Fig. 1. Apparatus.

A resistively heated oven was used for producing selenium vapour beam at a stable density of about  $10^{11}$  cm $^{-3}$ . A “hot”  $1.0 \times 1.0 \times 1.0$  mm $^3$  microchannel plate with the diameter of the single channel of 70  $\mu$ m, mounted at the end of the crucible, was used for the formation of the beam profile with

minimal angular divergence. The mechanical modulation of the beam enabled the background, arising from the electron scattering by residual gases, to be taken into account.

Selenium ions, created in the collision chamber, were extracted by applying the negative voltage to the plate electrode positioned close to the beam interaction region (see Fig. 1). The signal from it was registered by digital nanoamperemeter. A special attention was devoted to the optimal value of this voltage. By careful minimization of it to 1.0 – 1.5 V its effect on the incident electron beam inside the collision chamber was minimized and total collection of the formed ions was achieved. The experiment was fully automated. Both energy dependences of ion current and primary electron current were registered by a computer. Ionization efficiency was obtained by normalization of ion current on the incident electron current for each value of impact energy by using specially developed software.

The incident energy scale was calibrated for the value of the first 4p ionization threshold at 9.75 eV [12] at the point determined as the second derivative of the measured ion yield [13]. The energy scale was determined to an accuracy of 50 meV.

### Results and discussion

In Fig. 2 the measured ionization cross-section is shown along with the earlier ionization data [10]. The presence of a strong structure in the measured curve made the correct normalization of the experimental cross-section difficult. To avoid this effect the experimental data were put on the absolute scale by normalizing to the data of [10] below the ionization threshold at 9.75 eV [12], namely, at 9.4 eV. The relative uncertainties in the cross-section lie within 2%. In order to distinguish the observed structure, the linear fit of the data was subtracted from the original curve. This result is shown in the bottom of Fig. 2. As can be seen, there is a strong broad feature *A* with the “fine” structure *a-f* on the top and two well separated high energy features *g*, *h*. The energies of features *a* – *h* are listed in Table 1.

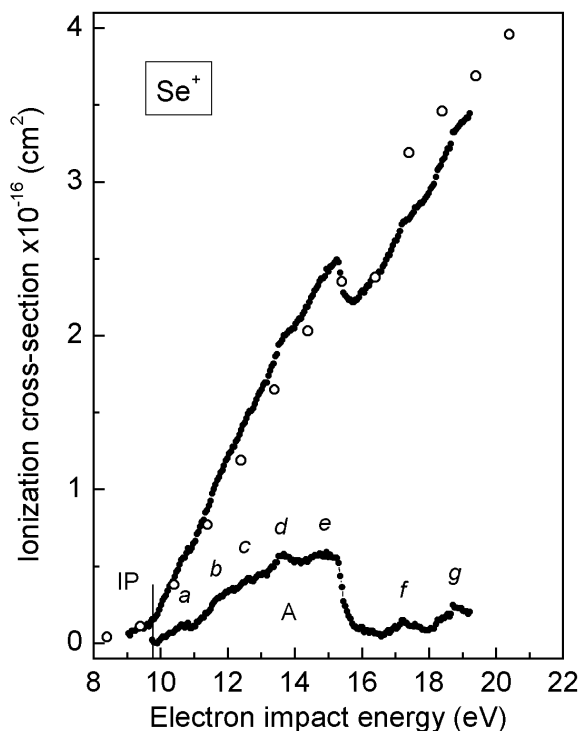


Fig. 2. Experimental electron-impact ionization cross-section of selenium: • – present data, ○ – data of [9]. The autoionization contribution is shown in the bottom (see the text).

Table 1. Energies (in eV) and identification of features observed in ionization cross-section of selenium

Feature	Energy	Identification
<i>a</i>	9.9 – 10.8	$4s^2 4p^3 ({}^2D_J) nd$ , $n = 4-6$ $4s^2 4p^3 ({}^2D_J) 7s$
<i>b</i>	11.3 – 12.2	$4s^2 4p^3 ({}^2D_J) nd$ , $n = 10-14$ $4s^2 4p^3 ({}^2P_{3/2}) nd$ , $n = 5, 6$ $4s^2 4p^3 ({}^2P_{3/2}) ns$ , $n = 7, 8$ $4s 4p^5 {}^3P^o$
<i>c</i>	12.6	$4s^2 4p^4 \rightarrow$ $4s^2 4p^2 n_1 l_1 n_2 l_2$ $4s^2 4p^4 \rightarrow$ $4s 4p^3 n_1 l_1 n_2 l_2$ $4s^2 4p^4 \rightarrow 4s^2 4p^3 nl$ $4s^2 4p^4 \rightarrow 4s 4p^4 nl$ (dipole forbidden)
<i>d</i>	13.0	
<i>e</i>	13.7	
<i>f</i>	14.9	
<i>g</i>	17.2	
<i>h</i>	18.8	

As it was mentioned above, the only data [8, 9] are known for selenium on the position of low-lying dipole allowed autoionizing states. We have used these data for the identification of the observed features *a* – *h*. As can be seen from Fig. 3 and Table 1, in the region of feature *a* between 9.9 and 10.8 eV the electron decay of five  $nd$  ( $n = 4-6$ ) and one  $7s$  configuration converging to the  ${}^2D_J$  limits may contribute to the measured ionization cross-section. The presence of this feature makes impossible the Wannier law application to the selenium ionization cross-section.

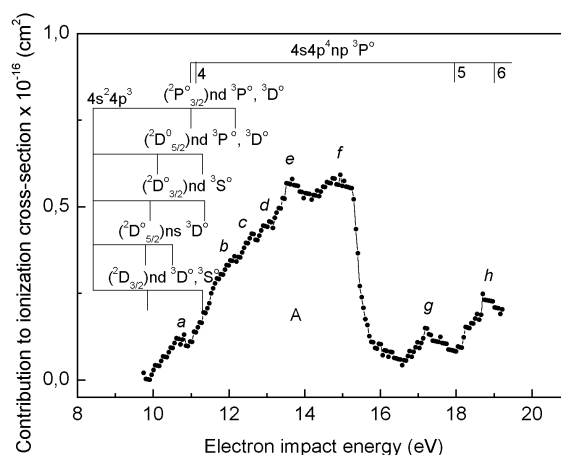


Fig. 3. Identification of the structure in the autoionization contribution to the ionization cross-section.

Considering the energy range 11.3–12.2 eV (feature *b*) shows that the higher terms ( $n > 10$ ) of the  $({}^2D_J) nd$  configurations, the  $({}^2P_{3/2}) nd$ ,  $ns$  configurations, and, to a lesser extent, the  $4s 4p^5 {}^3P^o$  level may contribute to the ionization of selenium.

As can be seen, in Fig. 3 there are no data on the presence of autoionizing levels in the region of features *c*, *d*, *e* and *f*. Meanwhile, just in this energy region the autoionization contribution achieves its maximum value of 19% (feature *e*) and, contrary to the features *a* and *b*, all these features possess remarkable resonance character. Therefore, we can suppose that both the observed features and the general enhancement of the cross-section are caused by the electron decay of autoionizing levels whose excitation from the ground state by photon impact is

forbidden and which possess strong negative-ion resonances at the excitation thresholds. Taking into account the data of [8, 9], such autoionizing levels may be assigned as belonging to the single- and two-electron configurations, namely,  $4s^2 4p^3 n l$ ,  $4s 4p^4 n l$ ,  $4s^2 4p^2 n_1 l_1 n_2 l_2$ , and  $4s 4p^3 n_1 l_1 n_2 l_2$ .

The last two features  $g$  and  $h$  are observed in our experimental data at the energies 17.2 and 18.8 eV. Their nature, similarly to the features  $c$ ,  $d$ ,  $e$ , and  $f$ , can be explained by excitation of dipole forbidden autoionizing levels with the above single- and two-electron configurations, especially  $4s 4p^4 n p$ .

In the region of the high-energy features  $g$  and  $h$  two window resonances were observed earlier [9]. The first of them  $4s 4p^3 5p^3 P^o$  at 17.94 eV coincides with the minimum of the cross-section around 18 eV. The second resonance  $4s 4p^3 6p^3 P^o$  at 19.01 eV is very close to the maximum of the feature  $h$  at 18.8 eV.

Considering the general behavior of the autoionization contribution in the region of the feature  $A$  one may conclude that the fast decrease of the cross-section after the feature  $f$  reflects the absence of autoionizing levels in the energy region 15.3–16.6 eV.

## Conclusions

We have presented the first data on the autoionization contribution to the near-threshold electron impact ionization cross-section of selenium over the impact energy region from the threshold up to 19.20 eV. The presence of the autoionizing states just above the ionization potential makes unable the use of Wannier threshold law application for selenium. The obtained data have revealed a dominant role of the dipole forbidden autoionizing configurations, tentatively assigned as  $s^2 p^3 ({}^2D, {}^2P) n l$  and  $s p^4 ({}^4P) n l$ , in the formation of this contribution in an energy region 13–15 eV. The resonance shape of the structure observed in the ionization cross-section points out the presence of strong negative-ion resonances at the excitation thresholds of the contributing autoionizing states. For the detailed analysis of the present data, an information on ejected-electron spectra in the region 0.1 – 9 eV is highly desirable.

## Acknowledgements

The authors are grateful to Prof. O.B. Shpenik and Dr. J.E. Kontros for favourable encouragement of work and help in performing the measurements.

## References

1. K.J.Nygaard, Phys. Rev. A 11, 1475 (1975).
2. S.J.Okudajra, J. Phys. Soc. Jap. 29, 409 (1970).
3. P.Marmet, M.Proulx, J. Phys. B 23, 549 (1990).
4. O.B.Shpenik, I.V.Chernishova, J.E.Kontros, Rad. Phys. Chem. 68, 277 (2003).
5. J.E.Kontros, L.Szoter, I.V.Chernishova, O.B.Shpenik, J. Phys. B 35, 2195 (2002).
6. D.Rassi, V.Pejcev, T.W.Ottley, K.J.Ross, J. Phys. B 10, 2913 (1977).
7. M.J.Evrij, A.A.Borovik (Jr.), L.L.Shimon, J.E.Kontros, A.A.Borovik, Nucl. Instrum. Meth. B. (2005) (in press).
8. A.M.Cantu, M.Mazzoni, Y.N.Yoshi, J. Opt. Soc. Am. 72, 1363 (1982).
9. S.T.Gibson, J.P.Greene, B.Ruscic, J.Berkowitz, J. Phys. B 19, 2841 (1986).
10. R.S.Freund, R.C.Wetzel, R.J.Shul, T.R.Hayes, Phys. Rev. A 41, 3575 (1990).
11. J.E.Kontros, L.Szótér, I.V.Chernyshova, O.B.Shpenik, J. Phys. B 35, 2195 (2002).
12. NIST Atomic Spectra Database Levels Data (2005): [http:// physics.nist.gov/cgi-bin/ASD/energy1.pl](http://physics.nist.gov/cgi-bin/ASD/energy1.pl).
13. F.P.Lossing, R.H.Emmel, B.G.Giessner, G.G.Meisels, J. Chem. Phys. 54, 5431 (1971).

## **ВНЕСКИ АВТОІОНІЗАЦІЙНИХ СТАНІВ У ПЕРЕРІЗ БІЛЯПОРОГОВОЇ ІОНІЗАЦІЇ СЕЛЕНУ ЕЛЕКТРОННИМ УДАРОМ**

**О.О.Боровик (мол.)<sup>1</sup>, Ф.Ф.Чіпєв<sup>2</sup>**

<sup>1</sup> Ужгородський національний університет,  
вул. Волошина 54, Ужгород, 88000  
e-mail: alex@aborovik.uzhgorod.ua

<sup>2</sup> Інститут електронної фізики НАН України,  
вул. Університетська 21, Ужгород, 88017  
e-mail: dep@mail.uzhgorod.ua

Використовуючи метод електронного й атомного пучків, що перетинаються, виміряно енергетичну залежність перерізу іонізації атомів селену від порогу процесу до 19.2 еВ. Дані одержано при енергетичній роздільній здатності 0.4 еВ. Вперше виявлено інтенсивну резонансну структуру як біля порогу, так і при більших енергіях зіткнень. Ідентифікація структури виявила домінуючу роль дипольно заборонених з основного стану переходів на автоіонізаційні конфігурації  $s^2p^3(^2D, ^2P)n/$  та  $sp^4(^4P)n/$  у збільшенні перерізу іонізації (до 19 %) в енергетичній області 13–15 еВ. Резонансний характер структури вказує на присутність негативних іонів у біляпороговому збудженні автоіонізаційних станів, що спричинюють збільшення перерізу іонізації.